Editors' Suggestion | Featured in Physics

Mechanics-based model for the cooking-induced deformation of spaghetti

Nathaniel N. Goldberg and Oliver M. O'Reilly*
Department of Mechanical Engineering, University of California, Berkeley, California 94720-1740, USA

(Received 9 August 2019; published 2 January 2020)

In this article, we propose a minimal model for the cooking-induced deformation of spaghetti and related food products. Our approach has parallels to the use of rod theories for the mechanics of slender bodies undergoing growth and is inspired by a wealth of experimental data from the food science literature. We use our model to investigate the cooking of a single strand of spaghetti confined to a pot and reproduce a curious three-stage deformation sequence that arises in the cooking process.

DOI: 10.1103/PhysRevE.101.013001

I. INTRODUCTION

The deformation of spaghetti is a topic that has received a surprising amount of attention in the mechanics community. Of particular interest has been the peculiar inability of a dry spaghetti strand to be broken into just two pieces, a puzzle that even caught the interest of the physicist Feynman. Noteworthy among several academic works on the problem is an elegant explanation by Audoly and Neukirch [1]. Mechanicians have also found interest in the problem of slurping a cooked noodle into one's mouth [2] as well as spitting it out [3].

The present paper studies the deformation of a single strand of spaghetti as it cooks. Our efforts are inspired by the following dinnertime experiment familiar to any home cook: Boil a pot of water and submerge a handful of dry spaghetti in it. A given strand will initially lie diagonally. After a short period of time, it will sag under the action of gravity as in Fig. 1(a). The strand will thereafter begin to settle along the bottom of the pot as it sags further, shown in Fig. 1(b). If sufficient out-of-plane constraint is imposed to prevent the noodle from tipping over, it will curl over onto itself as Fig. 1(c) depicts.

The natural question arises of what drives the spaghetti to deform as they are cooked. A naive answer would be that the cooking process weakens the noodles, allowing them to deform to an increasing extent under gravity. Such an explanation is certainly part of the story but does not account for a further experimental observation: take a few spaghetti out of the pot during the sagging stage and place them on a flat surface. If they have not been cooked for too long and have retained sufficient elasticity to overcome adhesion with the surface, one can observe a curvature to the noodles that persists even as they are left to dry. Thus, the cooking process endows the initially straight unstressed state of the spaghetti with curvature, a behavior which any attempt to model their deformation during cooking must take into account.

*oreilly@berkeley.edu

II. BACKGROUND

Before we begin our modeling efforts, we review the relevant scientific aspects of the production and cooking of spaghetti. Like most pasta, the predominant ingredient of spaghetti is semolina, a flour made from durum wheat (*Triticum durum*). In commercial pasta production, semolina is mixed with water to form a paste that is then extruded through a die to create the desired profile. The final step of production is drying, which is considered very challenging due to induced residual stresses and consequent cracking [5]. Many theoretical [6–8] and experimental [9–11] studies have explored methods of characterizing and improving the drying process.

The familiar task of cooking dried spaghetti involves little more than submerging the noodles in boiling water and waiting for a specified period of time. A typical spaghetti strand reaches the temperature of the surrounding water within a few seconds [12]. Water migration through the starch matrix occurs on a much slower timescale and in a strongly nonlinear fashion. Numerous experiments indicate that radial water imbibition in spaghetti is a non-Fickian process characterized by a sharp moving interface that separates a dry core from a hydrated annular region [13–16]. Hydration causes swelling in the annular zone which, in turn, increases the observed diameter and length. It also enables *starch depletion* in which small quantities of the starch component amylose leech into the surrounding water. As time progresses, the outermost portions of the hydrated zone where the water concentration is sufficiently high undergo *starch gelatinization*,[1] a chemical process that is responsible for the textural changes during cooking of starchy foods and is accompanied by additional swelling [17]. Spaghetti noodles are generally considered

[1]If the temperature is not above approximately 50 °C, gelatinization does not occur [17,18], and the spaghetti do not cook in the traditional sense, but they do still swell and soften considerably. Nevertheless, the texture is qualitatively different from that of spaghetti cooked in the usual way as the reader can experience by attempting to enjoy a plate of spaghetti that has been soaked for several hours in room-temperature water.

 ©2020 American Physical Society

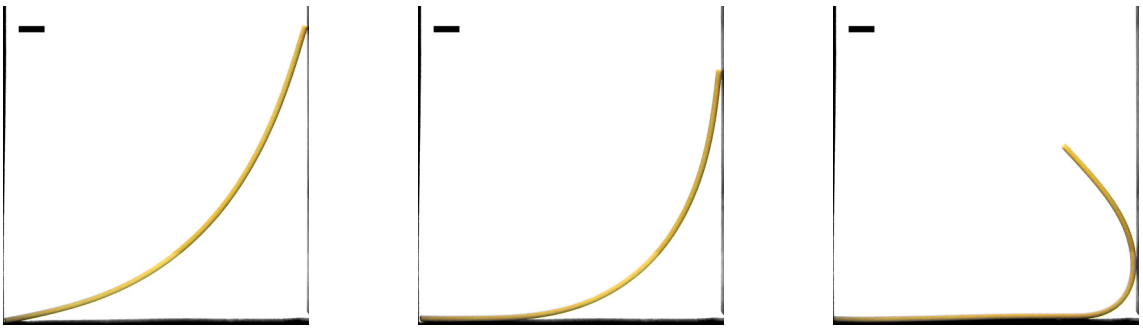

FIG. 1. Three stages of the cooking process. The black bar in the upper left corner of each image is 1 cm in length. These images of an experiment have been color corrected for clarity. A video of the experiment is included in the Supplemental Material for this paper [4]. (a) Stage 1: sagging, (b) Stage 2: settling, and (c) Stage 3: curling.

optimally cooked when the penetrative water front reaches the central axis [19].

Our goal is to develop a tractable model that reliably describes the purely macroscopic mechanical behavior of spaghetti as they are cooked. To this end, we hypothesize that the evolution of several mechanical properties during cooking is largely independent of the noodles' deformation. We, therefore, abstract away the numerous relevant phenomena described above and partially depicted in Fig. 2 by considering the following to be their mechanical resultant:

(1) the length is a prescribed function of time $L(t)$;
(2) the diameter is a prescribed function of time $d(t)$;
(3) the linear density is a prescribed function of time $\rho(t)$;
(4) the elastic modulus is a prescribed function of time $E(t)$; and
(5) the intrinsic curvature κ_0 evolves in time according to a flow rule depending on a time-dependent parameter $\alpha(t)$ to be discussed shortly.

The food science literature contains an abundance of data on the hydration of initially dry spaghetti under various conditions. The Appendix contains details about how we use these data to inform our prescriptions for Postulates 1–4 listed above. We must postpone discussion of Postulate 5 until after the model has been introduced.

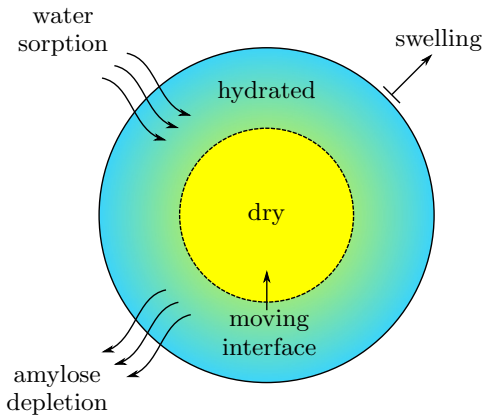

FIG. 2. The effect of hydration on a typical spaghetti strand's cross section.

III. MODEL DEVELOPMENT

We first develop a framework for studying the cooking-induced deformation of spaghetti under general planar circumstances and then specialize by investigating the three-stage deformation sequence shown in Fig. 1. Our approach is based on Euler's *elastica* and draws inspiration from work on the mechanics of growing rods [20–22]. We note that an extension to spatial deformations is readily achieved by introducing additional kinematic quantities in the same vein as Kirchhoff's rod theory and its generalizations [22–24].

A. Preliminaries

Consider an inextensible elastic rod (modeling a spaghetti noodle) described at time t by the current configuration $\mathcal{L}$ with $t = 0$ denoting the instant cooking of the rod begins. By conceptually removing all of the forces applied to $\mathcal{L}$ at time t, we generate the reference configuration $\mathcal{L}_0$.[2] Material points along $\mathcal{L}$ are marked with an arc-length coordinate $s \in (0, L(t))$. As the length $L(t)$ is treated as being known *a priori*, it will be occasionally convenient to mark material points instead by the dimensionless arc-length $z := s/L(t) \in (0, 1)$. Introducing the fixed Euclidean basis $\{\mathbf{E}_1, \mathbf{E}_2, \mathbf{E}_3\}$, the placement of a material point corresponding to the dimensionless arc-length z is

$$\mathbf{r} = \tilde{\mathbf{r}}(z, t) = \tilde{x}(z, t)\mathbf{E}_1 + \tilde{y}(z, t)\mathbf{E}_2. \tag{1}$$

It is convenient to introduce an angle θ from the horizontal at each point along the rod, i.e.,

$$\cos\theta = \frac{\partial x}{\partial s} \quad \text{and} \quad \sin\theta = \frac{\partial y}{\partial s}. \tag{2}$$

The *signed curvature* of $\mathcal{L}$ is then $\kappa = \partial\theta/\partial s$. An analogous procedure defines the signed curvature of $\mathcal{L}_0$, known as the *intrinsic* signed curvature and denoted by κ_0.

Two types of internal forces act on the *elastica*: contact forces $\mathbf{n}$ and contact moments $\mathbf{m}$. The former have the relevant

[2]Whereas works in the growth and plasticity literature draw a distinction between the reference configuration and the so-called *growth* or *intermediate* configuration obtained by unloading the current configuration, such a formalism is not required here.

components $n_1 = \mathbf{n}\cdot\mathbf{E}_1$ and $n_2 = \mathbf{n}\cdot\mathbf{E}_2$, whereas the latter have just $m = \mathbf{m}\cdot\mathbf{E}_3$. Applied forces and moments act in a distributed sense on the rod, the only such force in the present case being the gravitational force per unit length $-\rho g\mathbf{E}_2$.

The constitutive response of an inextensible *elastica* depends on the flexural rigidity EI which can be regarded either as a constitutive parameter in its own right, or, under certain circumstances, the product of the material's elastic modulus E and the cross section's second moment of area I.

When the intrinsic curvature κ_0 at a given time is known and quasistatic conditions prevail, the following equations fully determine the forces acting on, and the current position of, the rod at said time [23]:

$$n_1' = 0, \tag{3a}$$

$$n_2' = \rho g, \tag{3b}$$

$$m' = n_1 \sin\theta - n_2\cos\theta, \tag{3c}$$

$$\theta' = \kappa_0 + \frac{m}{EI}, \tag{3d}$$

$$x' = \cos\theta, \tag{3e}$$

$$y' = \sin\theta, \tag{3f}$$

where $(\,)' = \partial(\,)/\partial s$. At any given point $s = \beta$ on the rod where θ' is discontinuous or a singular force $\mathbf{F}_\beta$ acts, the following set of jump conditions must be satisfied [23]:

$$[\![\mathbf{n}]\!]_\beta + \mathbf{F}_\beta = \mathbf{0}, \tag{4a}$$

$$[\![m]\!]_\beta = 0. \tag{4b}$$

The rod in question does not suffer kinks, so $\mathbf{r}'$ and, consequently, θ are continuous functions of s.

Equations (3a) and (3b) are the projections of the balance of linear momentum onto $\mathbf{E}_1$ and $\mathbf{E}_2$, respectively, whereas Eq. (3c) is the projection of the balance of angular momentum onto $\mathbf{E}_3$. Equation (3d) is the constitutive law for the moment m. Lastly, Eqs. (3e) and (3f) are collectively the definition of angle θ. Importantly, for numerical implementation, Eqs. (3) are ordinary differential equations in the canonical form $\mathsf{u}' = \mathsf{f}(\mathsf{u}, s; t)$, the dependence on t being only parametric.

B. Flow rule

It remains to be discussed how one would come to know $\kappa_0 = \tilde{\kappa}_0(z,t)$. Imagine that the rod is sitting at time $t + \Delta t$, just having updated its length to $L(t+\Delta t)$, its diameter to $d(t+\Delta t)$, its density to $\rho(t+\Delta t)$, and its elastic modulus to $E(t+\Delta t)$ as dictated by the cooking process. If $m = \tilde{m}(z,t)$ is large enough in magnitude[3] at a given z, the hydrated annulus depicted in Fig. 2 can undergo a certain amount of flow, which causes the rod to behave as a viscoelastic solid in bulk despite its purely elastic inner core. We might reasonably assume that κ_0 increments by an amount instantaneously proportional to $m = EI(\kappa - \kappa_0)$ and, hence, to the strain $\kappa - \kappa_0$, i.e.,

$$\kappa_0(z, t+\Delta t) \approx \kappa_0(z,t) + \alpha(t)\Delta t[\kappa(z,t) - \kappa_0(z,t)]. \tag{5}$$

[3]No yield criterion is used in our computations in the spirit of simplicity.

In the limit $\Delta t \to 0$, we find

$$\dot{\kappa}_0 = \alpha(t)(\kappa - \kappa_0), \tag{6}$$

which was first introduced in the context of the growth of a plant stem by Goldstein and Goriely [25]. A suitable prescription for $\alpha(t)$ is discussed in the Appendix.

C. Numerical implementation

Given suitable initial and boundary conditions as well as prescriptions for $L(t)$, $d(t)$, $\rho(t)$, $E(t)$, and $\alpha(t)$, Eqs. (3) and (6) form the complete set of equations describing general deformations of a single spaghetti noodle during cooking. Note that Eqs. (3), which we previously noted are of the form $\mathsf{u}' = \mathsf{f}(\mathsf{u}, s; t)$, contain no time derivatives. In fact, the only time derivative among the governing equations occurs in the flow rule (6). It is, therefore, particularly straightforward to implement an explicit semidiscretization scheme in which a series of static problems are solved at discrete instances in time.

We introduce the discretization $t \to \{0, t_1, \ldots, t_k, \ldots, t_N\}$ and let u_k denote the approximate solution vector at time step k. In order to determine u_{k+1}, we first update the approximation to κ_0 by an approximation to the flow rule (6),

$$\tilde{\kappa}_{0,k+1}(z) = \tilde{\kappa}_{0,k}(z) + \alpha(t_k)\Delta t_k\left[\frac{\partial\theta_k}{\partial s}(z) - \kappa_{0,k}(z)\right], \tag{7}$$

where $\Delta t_k = t_{k+1} - t_k$. Once $\kappa_{0,k+1}$ is known, $\mathsf{u}_{k+1}' = \mathsf{f}(\mathsf{u}_{k+1}, s; t_{k+1})$ can be solved using any one of the many numerical techniques for ordinary differential equation boundary value problems. We use MATLAB's BVP4C routine.

IV. APPLICATION TO A SINGLE STRAND

We now apply our model to the specific situation shown in Figs. 1 and 3 in which a noodle confined to a transparent planar pot of width D hydrates with time. The purpose of our analysis is not to capture every relevant effect but rather to reproduce the core behavior of the noodle. As such, we make three key simplifying assumptions that imply certain boundary conditions in the following:

(1) the endpoint $s = 0$ remains pinned for all time;
(2) there is no adhesion or friction between the spaghetti and the pot; and
(3) the thickness of the spaghetti strand is negligible.

A careful review of the video provided in the Supplemental Material [4] shows that each of these assumptions is violated to a certain extent. However, we demonstrate that, even when we take them for granted, our model faithfully reproduces the primary features of the three-stage deformation sequence.

A. Stage one: Sagging

In the sagging stage [cf. Fig. 3(a)], the spaghetti strand is pinned at the left end and free to slide vertically at the right under the action of gravity. We, therefore, have the boundary conditions,

$$\begin{aligned} m &= 0, \\ x &= 0, \quad \text{at } s = 0, \\ y &= 0. \end{aligned} \tag{8}$$

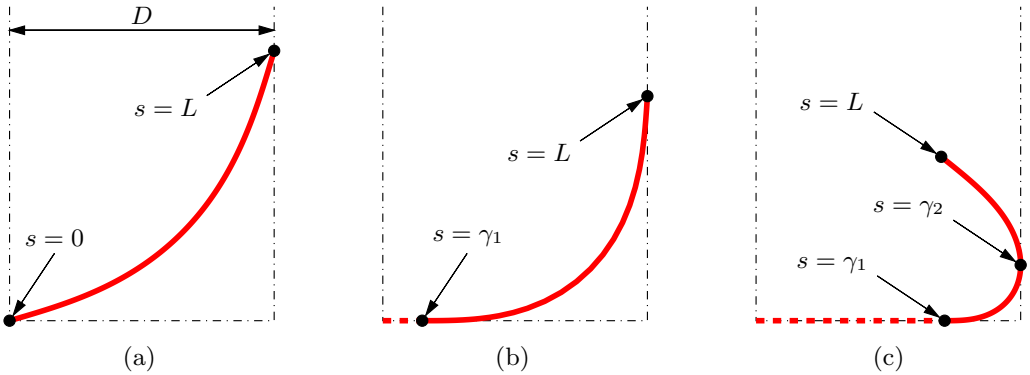

FIG. 3. Images of the deformed rod at each of the three stages of the simulated process: (a) sagging, (b) settling, and (c) curling. The points $s = 0$, $s = \gamma_1$, $s = \gamma_2$, and $s = L$ are highlighted. The images in this figure should be compared to the experimental results shown in Fig. 1.

and

$$\begin{aligned} n_2 &= 0, \\ m &= 0, \quad \text{at } s = L, \\ x &= D. \end{aligned} \tag{9}$$

The governing equations can be solved precisely in the manner discussed in Sec. III C, subject to the boundary conditions (8) and (9). Sagging is over once $\theta = 0$ at $s = 0$.

B. Stage two: Settling

The settling stage of the deformation [cf. Fig. 3(b)] sees the noodle split into two segments separated by the *a priori* unknown point $s = \gamma_1$. The segment $(0, \gamma_1)$ lies flat on the bottom of the pot with its left end still pinned in the corner. It is vital to note that, although $\kappa = 0$ in $(0, \gamma_1)$, $\kappa_0 \neq 0$ as the intrinsic curvature continues to evolve according to Eq. (6) and, hence, $m = -EI\kappa_0 \neq 0$ at $s = \gamma_1$.

Although the shape of the rod in $(0, \gamma_1)$ is known trivially, its shape in (γ_1, L) must be determined by solving $\mathsf{u}' = \mathsf{f}(\mathsf{u}, s; t)$ together with the flow rule (6). The principal difficulty in doing so can be traced to the fact that the domain on which the problem is to be solved is variable. One method of overcoming such difficulties is defining a new dependent variable,

$$q = \frac{s - \gamma_1}{L - \gamma_1}, \tag{10}$$

and noting that

$$\mathsf{u}' = \frac{1}{L - \gamma_1} \frac{d\mathsf{u}}{dq}. \tag{11}$$

Hence, we solve the equations,

$$\frac{d\mathsf{u}}{dq} = (L - \gamma_1)\mathsf{f}(\mathsf{u}, s; t), \tag{12}$$

on $q \in (0, 1)$ alongside the flow rule (6), substituting $s = \gamma_1 + q(L - \gamma_1)$ where necessary. We require the boundary conditions,

$$\begin{aligned} m &= -EI\kappa_0, \\ \theta &= 0, \\ x &= \gamma_1, \\ y &= 0, \end{aligned} \quad \text{at } q = 0, \tag{13}$$

in addition to

$$\begin{aligned} n_2 &= 0, \\ m &= 0, \quad \text{at } q = 1, \\ x &= D. \end{aligned} \tag{14}$$

Using the semidiscretization technique discussed previously, we have six scalar Eqs. (12) to solve as well as one unknown parameter γ_1 to determine, all subject to seven boundary conditions (13) and (14). Again, such a task is readily handled by a solver, such as BVP4C. Once $\theta = \pi/2$ at $q = 1$, the settling stage is considered complete.

C. Stage three: Curling

Three distinct sections emerge during curling [cf. Fig. 3(c)]. In addition to the familiar $(0, \gamma_1)$, there are (γ_1, γ_2) and (γ_2, L), γ_2 being the as-of-yet unknown point where the spaghetti strand touches the right wall, which can be determined in several ways.

One method, similar to that employed for the settling stage, involves writing the governing equations for both segments (γ_1, γ_2) and (γ_2, L), then performing two changes of variables—one on each set of equations—that make the new domain (0,1). However, such a method is cumbersome as it doubles the number of equations to be solved.

An alternative method is to consider a multipoint boundary value problem defined on $(\gamma_1, \gamma_2) \cup (\gamma_2, L)$. With the change in variables (10), the domain becomes $(0, G) \cup (G, 1)$, where G is the image of γ_2, which, like γ_1, is unknown *a priori*. The solution must satisfy the boundary conditions,

$$\begin{aligned} m &= -EI\kappa_0, \\ \theta &= 0, \\ x &= \gamma_1, \\ y &= 0, \end{aligned} \quad \text{at } q = 0 \tag{15}$$

interface conditions,

$$\begin{aligned} \theta &= \pi/2, \\ x &= D, \\ [\![n_2]\!] &= 0, \\ [\![m]\!] &= 0, \\ [\![\theta]\!] &= 0, \\ [\![x]\!] &= 0, \end{aligned} \quad \text{at } q = G, \tag{16}$$

and additional boundary conditions,

$$\begin{aligned} n_1 &= 0, \\ n_2 &= 0, \quad \text{at } q = 1, \\ m &= 0. \end{aligned} \tag{17}$$

One then ignores a single condition, say $\theta = \pi/2$ at $q = G$, and treats G as a known value to be iterated over until said suppressed boundary condition is satisfied to a chosen tolerance. Such a method can once again be implemented in MATLAB with BVP4C.

Once the rod has curled over on itself enough, it tends to begin to pull on the wall. To accommodate this, we simply release all conditions at γ_2 and use the same numerical technique as for the settling stage, albeit with the boundary conditions (17) at $q = 1$ rather than (14). When the endpoint $q = 1$ reaches $y = 0$, we assume that the noodle-to-noodle adhesion is strong enough that the endpoint is thereafter essentially fixed in this position. We consider the curling stage complete when any part of the rod re-initiates contact with the wall at $x = D$.

D. Results

To demonstrate the predictive capacity of our model, we took a time-lapse video of a spaghetti noodle hydrating over the course of approximately 2 h in room-temperature water (20 °C). The purpose of performing the experiment at room temperature rather than in proper cooking conditions was to simplify the experimental apparatus required. It should be noted that a qualitatively similar deformation sequence can be observed in spaghetti placed in boiling water, although imaging such an experiment is more challenging. The noodle was selected at random from a package of Trader Joe's brand spaghetti. The selected strand had an initial diameter of approximately 1.5 mm and was cut to a length of 17.5 cm. Snapshots were taken at intervals of 15 s, and the position of the right endpoint monitored using the open-source software TRACKER.

Simulations were performed according to the procedure outlined in Secs. III C and IV. As further discussed in the Appendix, prescriptions for $L(t)$, $d(t)$, and $\rho(t)$ were extracted from the food science literature, whereas $E(t)$ and $\alpha(t)$ were prescribed to be logistic functions and their parameters tuned to achieve qualitative agreement with experiment. In particular, the parameters t_0, τ, and α_∞ were varied.

Figure 4 compares the experimental measurements to the results of the model. The full time-lapse video with the numerical results superimposed can be found in the Supplemental Material [4].

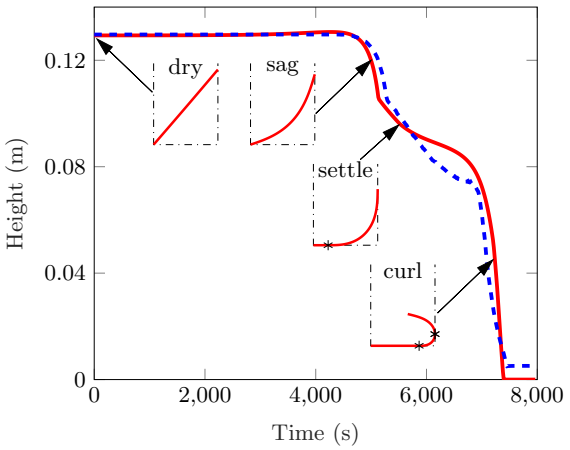

FIG. 4. Evolution of the height $y(L)$ of the right endpoint of a spaghetti noodle according to the model (solid curve) and experiment (dashed curve). The inset images show typical shapes predicted by the model during each stage of the deformation. Asterisks are used to distinguish the points $s = \gamma_1$ and $s = \gamma_2$. A video comparing the experiment to the simulation can be found in the Supplemental Material accompanying this paper [4].

V. CONCLUSION

In this paper, we have developed a rod-based model for spaghetti undergoing cooking or similar hydration processes and applied it to the special problem of a single strand being soaked in room-temperature water while confined to a pot. We have demonstrated both experimentally and numerically that the noodle's peculiar ability in this case to develop intrinsic curvature allows it to curl over on itself, evolving toward a configuration that is considerably more geometrically complex than its starting state. Our model was shown to provide good agreement with experimental results both qualitatively and quantitatively, despite the fact that it neglects effects, such as friction, adhesion, and inertia.

Several areas exist for improvement of the present model. Further incorporating concepts from the literature on the mechanics of growth would provide valuable improvements to our constitutive assumptions as would additional experiments on the bending of spaghetti at various temperatures and cook times. Additionally, one could adapt the discrete elastic rod numerical framework to take the essential features of our approach into account thereby reducing the considerable theoretical effort required to formulate specific boundary value problems.

Aside from being of theoretical interest to the mechanics community, our model might be of use in commercial food production as a means of quantifying the degree of cooking

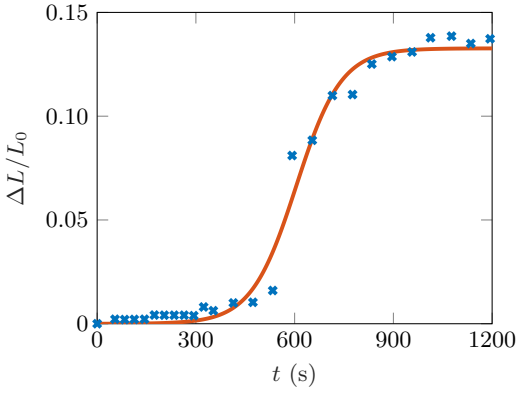

FIG. 5. Experimental length strain versus time at 20 °C as reported by Del Nobile and Massera [27]. A fit based on a logistic curve is superimposed on the data.

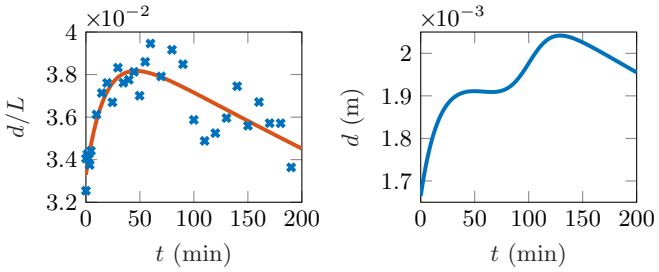

FIG. 6. Left: experimental time-aspect ratio relationship at 20 °C according to Del Nobile and Massera [27] with a superimposed two-term exponential fit. Right: diameter d as a function of time as calculated from the two-term exponential fit in combination with the logistic curve fit for ΔL in Fig. 5.

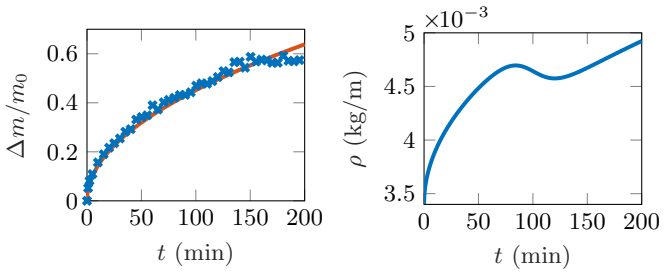

FIG. 7. Left: mass increase versus time as reported by Del Nobile and Massera [27] with our own square-root fit superimposed. Right: linear density as a function of time as computed from using the square-root fit with $m_0 = 0.1702$ g in combination with Fig. 5 with $L_0 = 4.71$ cm.

of noodles by way of merely observing their deformed shape. Future research could extend our modeling approach to spatial deformations of spaghetti or even to the deformation of shell-like pasta products, such as lasagna or rigatoni.

ACKNOWLEDGMENTS

The work of N.N.G. was supported by a Berkeley Fellowship for Graduate Study from the University of California, Berkeley. Additional support for N.N.G. was provided by a National Defense Science and Engineering Graduate Fellowship.

APPENDIX: TIME EVOLUTION OF L, d, ρ, E, AND α

Let us begin with $L(t)$ and $d(t)$, restricting attention to hydration at room-temperature (20 °C). Several studies, generally performed by placing short spaghetti strands in thermally controlled baths, have shown a qualitatively sigmoidal time-length relationship [18,26]. Figure 5 shows data by Del Nobile and Massera [27] together with a logistic fit of our own. Direct measurements of the diameter as a function of cooking time are absent from the aforementioned publication. However, it does contain data on the diameter-to-length aspect ratio as a function of time. Knowing the initial length of the authors' samples, the diameter-versus-time relationship can be backcalculated. Figure 6 shows the result of such a calculation.

Additional data are available on the mass increase-versus-time relationship to which a square-root fit appears to be a suitable model. Taking the previously obtained fit for $L(t)$, it is possible to compute of $\rho(t)$ from the mass data. The result of this calculation is shown in Fig. 7.

Unfortunately, the literature on spaghetti cooking appears not to contain any data on the evolution of the elastic modulus E at 20 °C. Absent more definitive motivation, we appeal to the approximately sigmoidal data collected by Cafieri *et al.* at 100 °C [28] and choose a logistic form for $E(t)$:

$$E(t) = E_0 e^{-t/\tau} \frac{1 + e^{t_0/\tau}}{1 + e^{-(t-t_0)/\tau}}, \tag{A1}$$

where $E_0 > 0$, $t_0 \geqslant 0$, and $\tau > 0$ are parameters that must be prescribed or determined from experiment. We note from Eq. (A1) that $E(t) \to 0$ as $t \to \infty$ as a dry spaghetti noodle is much stiffer than a fully hydrated one, i.e., $E(\infty)/E_0 \ll 1$.

A sensible form of the time-dependent flow rule parameter $\alpha(t)$ would have $\alpha(0) = 0$ due to the dry strand being incapable of viscoplastic flow. Furthermore, it would increase in time as more and more of the cross section becomes hydrated, eventually settling at a value such that $1/\alpha$ is on the order of the characteristic relaxation time of maximally hydrated spaghetti. For the sake of simplicity, we choose a logistic curve with the same timescale and offset as Eq. (A1), namely,

$$\alpha(t) = \alpha_\infty \frac{1 - e^{-t/\tau}}{1 + e^{-(t-t_0)/\tau}}, \tag{A2}$$

with $\alpha_\infty > 0$ being a phenomenological parameter.

[1] B. Audoly and S. Neukirch, Phys. Rev. Lett. **95**, 095505 (2005).
[2] G. F. Carrier, Am. Math. Mon. **56**, 669 (1949).
[3] L. Mansfield and J. G. Simmonds, J. Appl. Mech. **54**, 147 (1987).
[4] See Supplemental Material at http://link.aps.org/supplemental/10.1103/PhysRevE.101.013001 for video comparison of experiment and model.
[5] H.-D. Belitz, W. Grosch, and P. Schieberle, *Food Chemistry*, 4th ed. (Springer, Berlin, 2009).
[6] J. De Temmerman, P. Verboven, J. A. Delcour, B. Nicolaï, and H. Ramon, J. Food Eng. **86**, 414 (2008).
[7] G. Ponsart, J. Vasseur, J. M. Frias, A. Duquenoy, and J. M. Méot, J. Food Eng. **57**, 277 (2003).
[8] M. Migliori, D. Gabriele, B. de Cindio, and C. M. Pollini, J. Food Eng. **69**, 387 (2005).
[9] B. P. Hills, J. Godward, and K. M. Wright, J. Food Eng. **33**, 321 (1997).
[10] K. M. Waananen and M. R. Okos, J. Food Eng. **28**, 121 (1996).
[11] B. Cuq, F. Gonalves, J. Franois Mas, L. Vareille, and J. Abecassis, J. Food Eng. **59**, 51 (2003).
[12] A. Tesi, M. Primicerio, and A. Fasano, Networks Heterogen. Media **6**, 37 (2011).

[13] D. Bernin, T. Steglich, M. Röding, A. Moldin, D. Topgaard, and M. Langton, Food Res. Int. **66**, 132 (2014).
[14] M. A. Del Nobile and M. Massera, Cereal Chem. **77**, 615 (2000).
[15] B. P. Hills, F. Babonneau, V. M. Quantin, F. Gaudet, and P. S. Belton, J. Food Eng. **27**, 71 (1996).
[16] A. K. Horigane, S. Naito, M. Kurimoto, K. Irie, M. Yamada, H. Motoi, and M. Yoshida, Cereal Chem. **83**, 235 (2006).
[17] D. Lund and K. J. Lorenz, Crit. Rev. Food Sci. Nutr. **20**, 249 (1984).
[18] M. A. Del Nobile, G. G. Buonocore, A. Panizza, and G. Gambacorta, J. Food Sci. **68**, 1316 (2003).
[19] S. Chillo, M. Iannetti, V. Civica, N. Suriano, M. Mastromatteo, and M. A. Del Nobile, J. Food Eng. **94**, 222 (2009).
[20] N. A. Faruk Senan, O. M. O'Reilly, and T. N. Tresierras, J. Mech. Phys. Solids **56**, 3021 (2008).
[21] O. M. O'Reilly and T. N. Tresierras, Int. J. Solids Struct. **48**, 1239 (2011).
[22] A. Goriely, *The Mathematics and Mechanics of Biological Growth*, Interdisciplinary Applied Mathematics (Springer-Verlag, New York, 2017).
[23] O. M. O'Reilly, *Modeling Nonlinear Problems in the Mechanics of Strings and Rods*, Interaction of Mechanics and Mathematics (Springer, Cham, Switzerland, 2017).
[24] S. S. Antman, *Nonlinear Problems of Elasticity*, Applied Mathematical Sciences (Springer-Verlag, New York, 2005).
[25] R. E. Goldstein and A. Goriely, Phys. Rev. E **74**, 010901(R) (2006).
[26] S. Chillo, J. Laverse, P. M. Falcone, A. Protopapa, and M. A. Del Nobile, J. Cereal Sci. **47**, 144 (2008).
[27] M. A. Del Nobile and M. Massera, J. Food Eng. **55**, 237 (2002).
[28] S. Cafieri, M. Mastromatteo, S. Chillo, and M. A. Del Nobile, J. Food Eng. **100**, 336 (2010).